Thermal inhibition of high-power second-harmonic generation in periodically poled Li Nb O 3 and Li Ta O 3 crystals

Oleg A. Louchev, Nan Ei Yu, Sunao Kurimura, and Kenji Kitamura

Citation: Applied Physics Letters **87**, 131101 (2005); doi: 10.1063/1.2056593
View online: http://dx.doi.org/10.1063/1.2056593
View Table of Contents: http://scitation.aip.org/content/aip/journal/apl/87/13?ver=pdfcov
Published by the AIP Publishing

Thermal inhibition of high-power second-harmonic generation in periodically poled $LiNbO_3$ and $LiTaO_3$ crystals

Oleg A. Louchev,[a] Nan Ei Yu,[b] Sunao Kurimura, and Kenji Kitamura
Advanced Materials Laboratory, National Institute for Materials Science, 1-1 Namiki, Tsukuba, Ibaraki 305-0044, Japan

(Received 2 May 2005; accepted 2 August 2005; published online 19 September 2005)

A coupled thermo-optical model shows strong thermal inhibition of second-harmonic generation (SHG) in periodically poled (PP) $LiNbO_3$ (PPLN) and stoichiometric $LiTaO_3$ (PPSLT) crystals. Three-dimensional simulations performed for a 1.064 μm fundamental wavelength pulsed nanosecond laser beam 150 μm in radius show the onset of significant temperature nonuniformities along and across the irradiated zone, and strong thermal dephasing and inhibition of SHG in these crystals for input powers >10 W. PPSLT is found to have a significant advantage over PPLN due to the higher heat conductance, decreasing these temperature nonuniformities and allowing one to maintain the irradiated zone within the corresponding SHG temperature tolerance range ($\Delta T \approx 3$ K). © *2005 American Institute of Physics*. [DOI: 10.1063/1.2056593]

Second-harmonic generation (SHG) using quasi-phase matching (QPM) in periodically poled (PP) crystals[1] has shown significant progress over the last decade, and continues to remain in the focus of research efforts aimed towards greater efficiency devices working at higher input powers.[2–11] PP $LiNbO_3$ (PPLN) and PP stoichiometric $LiTaO_3$ (PPSLT) remain among the best SHG materials due to their high second order susceptibility.[12] Nevertheless, efforts to use these and also similar crystals for high power SHG encounter the problem of efficiency loss, difficult temperature tuning and thermally induced long term degradation.[11] In this letter we consider the optical problem of SHG in PPLN and PPSLT crystals coupled with a three-dimensional (3D) heat transfer model which shows the onset of increasing thermal dephasing and SHG efficiency loss for a 1.06 μm fundamental wavelength pulsed laser at input powers >10 W. Our study also shows that PPSLT crystals which have a lower value of effective nonlinearity, $d_{\text{eff}} \approx 10$ pm/V (compared with $d_{\text{eff}} \approx 16$ pm/V for LN), provide a significant advantage over PPLN due to two times higher heat conductance, 8.5 W/m K,[9] which becomes the critical parameter controlling SHG at high input powers.

We consider continuum-wave (cw) and nanosecond SH pulse generation in PP crystals schematically shown in Fig. 1. For the case of cw and nanosecond pulse SHG wave amplitudes can be considered in a slowly varying amplitude approximation. In formulating the problem we take into account (a) the square-wave periodicity of the effective nonlinearity coefficient as $d(z)=d_{\text{eff}}\text{sign}[\cos(2\pi z/\Lambda)]$ (where Λ is the QPM period), and (b) optical loss by linear absorption ($\alpha_j I_j$) and nonlinear two-photon absorption (βI_2^2). For any particular moment t and x-y input point at the front of the crystal the conversion mechanism for fundamental harmonic (FH, $i=1$) and second harmonic (SH, $i=2$) along the z coordinate is approximated by

$$\frac{dA_1}{dz} = \frac{8\pi i\omega_1^2}{k_1 c^2} d(z) A_2 A_1^* \exp(-i\Delta k z) - 0.5\alpha_1 A_1, \tag{1}$$

$$\frac{dA_2}{dz} = \frac{4\pi i\omega_2^2}{k_2 c^2} d(z) A_1^2 \exp(i\Delta k z) - 0.5(\alpha_2 + \beta^* A_2 A_2^*) A_2, \tag{2}$$

where $k_j = n_j\omega_j/c$ is the wave vector, $\Delta k = 2k_1 - k_2$ is the wave vector mismatch between FH and SH waves, $\beta^* = \beta n_2 c/2\pi$ and β is the two-photon absorption coefficient for SH.

The 3D and time-dependent distributions within the irradiated zone and at the crystal output are obtained by solving these equations with the following condition at $z=0$:

$$A_1 = \left[\frac{2\pi I_0 f_1(x,y) f_2(t)}{n_1 c}\right]^{1/2} \text{and } A_2 = 0, \tag{3}$$

where $f_1(x,y)=\exp[-(x^2+y^2)/r_0^2]$ is the input radial distribution of the laser beam (r_0 is the beam radius), $f_2(t)=1$ for cw laser and $f_2(t)=\exp[-(t-t_0)^2/\tau^2]$ is the time function for pulsed mode (2τ is the pulse duration time).

The local beam intensities along the direction z are associated with the wave amplitudes by

$$I_j(\mathbf{x},t) = \frac{n_j c}{2\pi} |A_j(\mathbf{x},t)|^2. \tag{4}$$

The values of refractive indices depend on the temperature $n_j(\lambda, T)$[12] and change the values of $k_j = n_j\omega_j/c$ and $\Delta k = 2k_1 - k_2$ defining solution of Eqs. (1)–(4). Thus, the above optics problem is coupled with T field inside the crystal (i =cr) and metal holder ($i=h$) described by a 3D equation

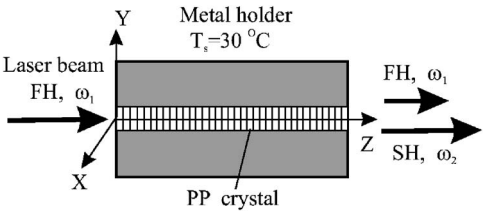

FIG. 1. Optical and thermal setup of SHG.

[a]Author to whom correspondence should be addressed; electronic mail: louchev.oleg@nims.go.jp
[b]Present address: Advanced Photonics Research Institute, Gwangju Institute of Science and Technology, Gwangju 500-712 Korea; electronic mail: neyu@gist.ac.kr

$$\rho_i C_i \partial T_i/\partial t = K_i \nabla^2 T_i + q_i(\mathbf{x},t), \tag{5}$$

where ρ_I, C_i, K_i are the densities, specific heats and heat conductances, respectively, of crystal and metallic holder. The external temperature of the assembly is assumed to be constant at $T=T_s$. At the front ($z=0$) and rear side ($z=L$) of the crystal holder we assume the heat exchange condition, i.e., $-K_i \nabla T_i = h(T_i - T_0)$, where $h \approx 10$ W/m^2 K is the heat exchange coefficient to air at $T_0=20$ °C.

For a cw laser the heat source distribution inside the PP crystal is defined by the derivative of the total beam intensity along the beam propagation direction z as

$$q_{\mathrm{cr}}(\mathbf{x},t) = -\frac{d}{dz}[I_1(\mathbf{x},t) + I_2(\mathbf{x},t)] = \alpha_1 I_1 + \alpha_2 I_2 + \beta I_2^2. \tag{6}$$

For a nanosecond pulse laser the quasi-state approximation using an averaged heat source in estimating the distribution defined by Eq. (6) can be used:

$$q_{\mathrm{cr}}(\mathbf{x},t) = \nu \int_{\Delta t} (\alpha_1 I_1 + \alpha_2 I_2 + \beta I_2^2) dt, \tag{7}$$

where Δt is the period used for the time integration of one laser pulse and ν is the laser pulse frequency. This approximation can be used for modes when the characteristic time of the temperature stabilization (for considered cases $\approx 0.1-1$ s) is much larger than the time defined as ν^{-1}.

In our study we use a finite-difference scheme combining (i) $30\times30\times20$ point grid for T field, (ii) $30\times30\times40\,000$ point grid for the wave amplitudes and intensities and (iii) 200 point time discretization for pulse duration time. The coupling of Eqs. (1)–(4) with T field via the temperature dependence of the refractive indices $n(\lambda,T)$,[12,13] k_j and Δk is obtained by linear interpolation of the T-field points along z. The discretization parameters are adjusted to maintain all integral energy balances within 1% accuracy. The optimal QPM periods for device temperature $T=30$ °C are $\Lambda = 2\pi/\Delta k = 6.84$ μm (LN) and $\Lambda = 2\pi/\Delta k = 8.02$ μm (SLT). For LN $d_{\mathrm{eff}} \approx 16$ pm/V[12] and for SLT $d_{\mathrm{eff}} \approx 10$ pm/V.[9] The heat conductance is $K_{\mathrm{cr}} \approx 4.6$ W/m K for LN[14] and $K_{\mathrm{cr}} \approx 8.5$ W/m K for SLT;[9] $C_{\mathrm{cr}}=650$ J/kg K and $\rho=4600$ kg/m^3 for LN; $C_{\mathrm{cr}}=410$ J/kg K and $\rho=7400$ kg/m^3 for SLT. For LN $\alpha_1 \approx 0.002$ cm^{-1}($\lambda_1=1.06$ μm), $\alpha_2 \approx 0.025-0.045$ cm^{-1}($\lambda_2=0.53$ μm) and $\beta = 2-5\times10^{-11}$ m/W.[12] Additionally, for LN the green-induced infrared absorption can provide significant crystal heating.[15,16] However, this detrimental effect is inhibited in Mg doped LN, and can be neglected for SLT, so is not included in our model.[16] For SLT crystals the values of α_1 and α_2 remain within ranges similar to LN.[15] For SLT the value of β has not yet been measured but it is expected to be lower than for LN. In our study we use the same set of absorption parameters for LN and SLT: $\alpha_1 = 0.002$ cm^{-1}, $\alpha_2 = 0.025$ cm^{-1} and $\beta = 5\times10^{-11}$ m/W.[12,15] The calculations are performed for $1\times1\times10$ mm crystals inside a $4\times4\times10$ mm Al holder for the following laser parameters: $\nu=50$ kHz, pulse input energy $Q_0=0.01-1$ mJ and power $W_0=\nu x Q_0=0.5-50$ W, beam radius $r_0=150$ μm and pulse duration time $2\tau=20$ ns.

Figure 2 shows SHG efficiency (W_2/W_0) versus input power W_0 for both materials. Dashed lines show W_2/W_0 at QPM temperature 30 °C, whereas the solid lines show W_2/W_0 after complete T-field stabilization. Both materials show similar behavior, i.e., an initial increase with increase in W_0 followed by sharp decrease and oscillations appearing with further increase in W_0. This complex behavior is due to the interference of two counteracting effects. The first one is the increase in W_2/W_0 with increase in W_0. However, the further increase in W_0 and W_2 increases absorption ($\alpha_2 I_2 + \beta I_2^2$) in the middle and rear of the crystals, leading to significant increase in T and in wave vector mismatch (Δk). This effect provides the oscillation shown in Fig. 2, which is typical for dependence of SHG efficiency on Δk. Figure 2 shows that the thermal inhibition of SHG for PPSLT takes place at significantly larger W_0. This is explained by two factors: (i) the temperature tolerance of PPSLT of ≈3.0 °C and (ii) the high heat conductance, 8.5 W/m K, which is about two times larger than that of LN. To outline the importance of these two factors we show in Figs. 3 and 4 the set of FH and SH intensities and temperature distributions calculated for $W_0=20$ for which the resulting SHG efficiency (Fig. 2 solid lines) is found to be ≈0.15 (PPLN) and ≈0.4 (PPSLT). In particular in Fig. 3 we show the initial and final distributions of FH and SH intensities along the beam propagation axis (z) for (a) PPLN and (b) PPSLT taken at the peak intensity of the pulse, and (c) initial and final T-field distributions for both materials. Figure 4 shows the radial distributions of the input FH intensity, the initial and final output

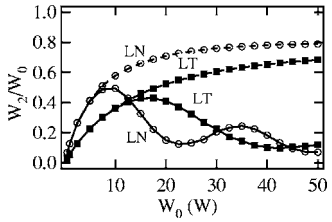

FIG. 2. SHG efficiency (W_2 is the output SH power and W_0 is the FH input power) vs input power simulated for PPLN (○) and PPLT (■) crystals: (i) broken lines correspond to the initial moment with initial uniform $T=30$ °C and (ii) solid lines—to the final T-field stabilization.

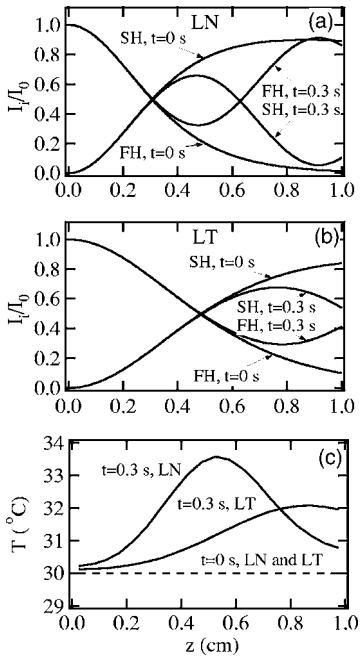

FIG. 3. Initial and final distributions along the beam propagation axis of FH and SH intensity for (a) PPLN, (b) PPLT with (c) corresponding temperature distributions.

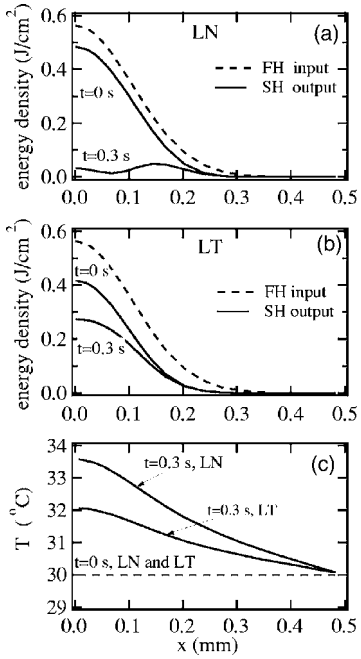

FIG. 4. Initial and final radial distributions of one laser pulse input FH and output SH energy densities for (a) PPLN, (b) PPLT together with (c) the corresponding temperature distributions having maximal ΔT across the laser beam (at $z=0.525$ cm for LN and $z=0.9$ for LT).

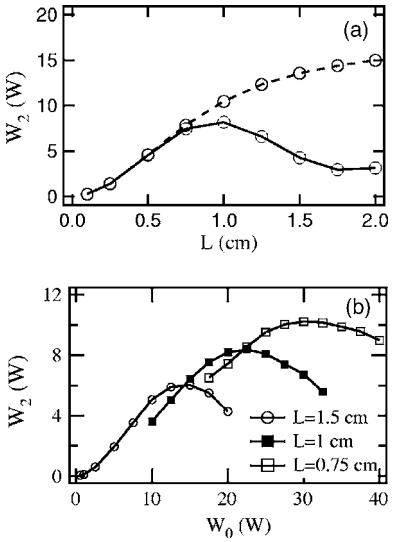

FIG. 5. Calculated maximums of the output SHG power for PPSLT as function: (a) $L(W_0=20$ W) at QPM temperature (broken) and after T-field stabilization (solid), and (b) W_0 for several values of L.

SH intensity for (a) PPLN, (b) PPSLT as well as (c) the initial and final radial temperature distributions for both materials. These figures reveal how the intensities and T fields evolve with time and why PPLN shows a dramatic fall in SHG efficiency (from ≈0.7 to ≈0.15) with T-field stabilization, whereas PPSLT continues to have reasonably high efficiency (≈0.4) even after T-field stabilization. That is, in the case of PPLN the temperature field is ≈3.5 °C over that of QPM and in major part of the irradiated zone the temperature tolerance semiwidth (1.7 °C from T of QPM) is exceeded. This causes thermal dephasing and significant change in I_1 and I_2 distributions along and across the beam propagation direction leading to the strong decrease of the output local, time and integral values of I_2. In contrast, in the case of PPSLT the final maximal increase in T is ≈2 °C over that of QPM and, hence, the significant part of the irradiated zone remains within the temperature tolerance range.

Thus, the larger heat conductance of PPSLT allows one to maintain the irradiated zone within the temperature tolerance range for larger input powers as compared with PPLN. Focusing now for the sake of brevity on PPSLT we show in Figs. 5(a) and 5(b) the absolute SHG output power W_2 as a function of (a) crystal length $L(W_0=20$ W) and (b) input power W_0 for several values of L. Figure 5(a) shows that for any W_0 there is an optimal crystal length providing maximal SH output. At QPM temperature the increase in L tends to increase W_2 (broken line). However, with increase in I_2 at the crystal middle and rear the SH absorption and related thermal effects interfere and decrease W_2 (solid line). Moreover, notwithstanding the fact that in a 1 cm PPSLT crystal the final SH intensity distribution [Fig. 3(b)] has a maximum at $z\approx0.75$ cm, the reduction of L from 1 to 0.75 cm leads, in fact, to a decrease in W_2 due to the nonlinearity of the problem. However, for LN the reduction of L from 1 to 0.5 cm [following Fig. 3(a)] increases W_2/W_0 and changes W_2 from ≈3 to ≈7.5 W. Figure 5(b) shows that the larger W_0 the smaller the length providing maximal SHG output due to decrease of the effective distance within which FH and SH fields exchange energy, $\ell \propto 1/d_{\text{eff}}I_0^{1/2}$.[1]

In conclusion, we have to note that the temperature nonuniformities revealed here create additional restrictions associated with thermal lensing effects destroying SHG device operation.[17] Hence, the heat conductance of the crystal becomes the critical parameter controlling SHG efficiency at high input powers; and PPSLT has a significant advantage over PPLN and similar SHG materials having lower heat conductance.

[1] J. A. Armstrong, N. Bloemberger, J. Ducuing, and P. S. Pershan, Phys. Rev. **127**, 1918 (1962).
[2] D. H. Jundt, G. A. Magel, M. M. Fejer, and R. L. Byer, Appl. Phys. Lett. **59**, 2657 (1991).
[3] V. Pruneri, S. D. Butterworth, and D. C. Hanna, Opt. Lett. **21**, 390 (1996).
[4] A. Englander, R. Lavi, M. Katz, M. Oron, D. Eger, E. Lebiush, G. Rosenman, and A. Skliar, Opt. Lett. **22**, 1598 (1997).
[5] G. D. Miller, R. G. Batchko, W. M. Tulloch, D. R. Weise, M. M. Fejer, and R. L. Byer, Opt. Lett. **22**, 1834 (1997).
[6] V. Pasiskevicius, S. Wang, J. A. Tellefsen, F. Laurell, and H. Karlsson, Appl. Opt. **37**, 7116 (1998).
[7] S. V. Popov, S. V. Chernikov, and J. R. Taylor, Opt. Commun. **174**, 231 (2000).
[8] K. Mizuuchi, A. Morikawa, T. Sugita, K. Yamamoto, N. Pavel, I. Shoji, and T. Taira, Jpn. J. Appl. Phys., Part 2 **42**, L1296 (2003).
[9] N. E. Yu, S. Kurimura, Y. Nomura, and K. Kitamura, Jpn. J. Appl. Phys., Part 2 **43**, L1265 (2004).
[10] M. Katz, R. K. Route, D. S. Hum, K. R. Parameswaran, G. D. Miller, and M. M. Fejer, Opt. Lett. **29**, 1775 (2004).
[11] Z. M. Liao, S. A. Payne, J. Dawson, A. Drobshoff, C. Ebbers, and D. Pennington, J. Opt. Soc. Am. B **21**, 2191 (2004).
[12] V. G. Dmitriev, G. G. Gurzayan, and D. N. Nikogosyan, *Handbook of Nonlinear Optical Properties* (Springer, Berlin, 1999).
[13] A. Bruner, D. Eger, M. B. Oron, P. Blau, M. Katz, and S. Ruschin, Opt. Lett. **28**, 194 (2003).
[14] V. V. Zhdanova, V. P. Klyuev, V. V. Lemanov, I. A. Smirnov, and V. V. Tikhonov, Sov. Phys. Solid State **10**, 1360 (1968).
[15] A. L. Alexandrovski, G. Foulon, L. E. Myers, R. K. Route, and M. M. Fejer, Proc. SPIE **3610**, 44 (1999).
[16] Y. Furukawa, K. Kitamura, A. Alexandrovski, R. K. Route, M. M. Fejer, and G. Foulon, Appl. Phys. Lett. **78**, 1970 (2001).
[17] S. A. Akhmanov, R. V. Khohlov, and A. P. Sukhorukov, in *Laser Handbook*, edited by F. T. Arecchi and E. O. Schulz-Dubois (North-Holland, Amsterdam, 1979), Vol. 2, pp. 1151–1228.